Ground Support 2026 - D Cumming-Potvin & J Wesseloo (eds.)
© 2026 Australian Centre for Geomechanics, Perth
doi:10.36487/ACG_repo/2625_05

Influence of dynamic test method on the performance of a mechanically anchored hybrid rockbolt

Rual Abreu [a,*], Cornelius Swart [a]

[a] *Normet, Australia*

Abstract

Dynamic rock reinforcement is a critical component of ground support strategies in high-stress underground mining environments, and requires a thorough understanding of how support systems respond under seismic loading. This paper investigates the dynamic performance of mechanically anchored hybrid rockbolts when subjected to both continuous-tube and split-tube laboratory testing configurations. It then explores how a hybrid bolt design can be adapted to include chemical anchorage to improve bolt performance in various loading scenarios and to increase installed bolt longevity.

Mechanically anchored hybrid bolts are typically designed for rapid, mechanised installation without the use of resin or grout. These systems comprise a yielding tendon integrated within a mechanically anchored friction unit and are installed using percussive force, followed by rotation of a nut to pretension the assembly and activate a mechanical expansion anchor. This bolt style offers an effective alternative to bonded anchors in conditions where resin or grout is impractical, while delivering improved installation efficiency and suitability across a wide range of ground conditions.

Dynamic rockbolts are commonly qualified using laboratory impact testing methods intended to simulate in situ seismic loading. The 2 principal approaches are:

- *continuous-tube, direct-impact testing which simulates rock mass strainburst behaviour*
- *split-tube, indirect impact testing which simulates block ejection scenarios.*

To date, published dynamic testing of hybrid bolts has overwhelmingly favoured continuous-tube methods, which align well with the design of hybrid bolts and their reliance on faceplate loading to activate the end-anchor and facilitate energy absorption through controlled tendon yielding.

Limited investigation has been conducted into the performance of mechanically anchored hybrid rockbolts under split-tube, block ejection, loading conditions. In this configuration, the friction unit can partially insulate the yielding tendon from the host-tube or rock mass displacement forces, disrupting the load path between the supported mass and the tendon. This can interfere with proper function of the bolt's wedge anchor and yielding mechanism. The bolt is then reliant on frictional slip or localised component failure of the friction unit before load transfer to the tendon and activation of the expansion anchor can occur.

The paper characterises the load transfer mechanisms acting on the yielding tendon under both dynamic test methods, compares the performance of a conventional hybrid bolt design in continuous- and split-tube configurations, and evaluates targeted design modifications intended to optimise load transfer in both loading scenarios. The outcomes demonstrate improved dynamic performance and repeatability, supporting broader qualification of hybrid bolts for a range of dynamic ground conditions.

Keywords: *dynamic ground support, hybrid rockbolt, yielding rockbolt, dynamic rockbolt testing*

[*] Corresponding author email address: rual.abreu@normet.com

1 Introduction

Mines are required to operate at ever increasing depths to reach deposits. As mining depth increases, so do in situ stresses. These field stresses increase approximately linearly with depth, resulting in significant stress concentrations around deep excavations. Shakeri et al (2026) say these elevated stresses often lead to localised brittle rock failure, such as rockbursts, as well as more global stress redistribution events such as mining-induced seismicity. Consequently, there is a fundamental shift in the performance requirement of rock reinforcement systems at depth, as these need to resist both high static loads as well as tolerate rock mass deformation and dynamic loading without loss of support confinement (Morissette & Hadjigeorgiou 2017).

Fully encapsulated dynamic resin bolts, such as the D Bolt® are well proven to provide optimal initial support capacity as well as dynamic capacity if loaded beyond yield (Li 2010). However, this class of rockbolt is dependent on the correct application of resin or grout to bond the anchor into the rock and is subject to chemical curing times and adequate encapsulation quality to achieve full support capacity. Performance of these systems are sensitive to borehole conditions, chemical quality, mixing, annus spacing and mixing technique, all of which greatly influences the system's performance (Hadjigeorgiou & Potvin 2011). This class of rockbolt remains highly effective in mines where conditions and operations are favourable, however there has been a sharp rise in the adoption of mechanically anchored hybrid rockbolts in operations where conditions are not well suited to fully encapsulated systems. These hybrid bolts provide instantaneous dynamic support capacity through mechanical anchorage into the rock, rather than chemical anchorage. They are less sensitive to optimal borehole conditions and do not require a curing time to lapse before full capacity is achieved, speeding up the support cycle time.

The construction of mechanically anchored dynamic hybrid rockbolts is inherently more complex than chemical anchors and the mechanical anchor can lead to localised stress concentrations in the borehole. These systems are also more susceptible to corrosion, which can rapidly erode bolt performance if not managed. Given the introduction of this bolt design is recent, there is little data available on the long-term reliability of these systems as permanent support and several studies are underway to better understand the benefits and trade-offs of this bolt class.

Much of this recent research has focused on understanding and quantifying the performance of these bolts during various loading scenarios and has suggested that mechanically anchored hybrid rockbolts are highly effective in managing rockbursts and tolerating shear loads (Cai & Kaiser 2022; Knox & Hadjigeorgiou 2025). This is because the anchorage mechanism and general design of hybrids bolts is well suited to situations where the primary load is applied to the faceplate, as is the case with rockbursts. In this loading scenario, the load is applied to the faceplate which transfers load directly onto the proximal end of the yielding tendon. The tendon resists this load by transferring the applied tension to the mechanical expansion anchor located towards the distal end of the bolt. The increase of load on the expansion anchor helps further expand the mechanism and increases its anchorage into the borehole.

There is, however, very little data available to inform how these bolts perform during block ejection loading scenarios where the primary load path is directed onto the friction anchor and not directly onto the faceplate. In this scenario, there is a significant depth of intact rock between the skin of the excavation and the fault in the rock, see length B of Figure 1. Anchorage of the hybrid bolt is then limited to the length of bolt remaining anchored into the competent rock, length A of Figure 1. If the rock below the fault is intact enough that the borehole maintains frictional anchorage along length B of the hybrid bolt, conflicting load paths act on the friction anchor because the anchored length A needs to resist tensile loads applied by length B and this load is transferred along the friction anchor, and not the internal tendon. Consequently, no increased load is passed via the tendon to the expansion anchor, and it does not increase its anchorage as the design intends.

In such a scenario, load would only transfer onto the faceplate and into the tendon if anchorage along length B is overcome and localised slippage occurs. Should anchorage along length B be greater than length A, the anchor would pull free from the rock before further activation of the mechanical expansion mechanism could occur.

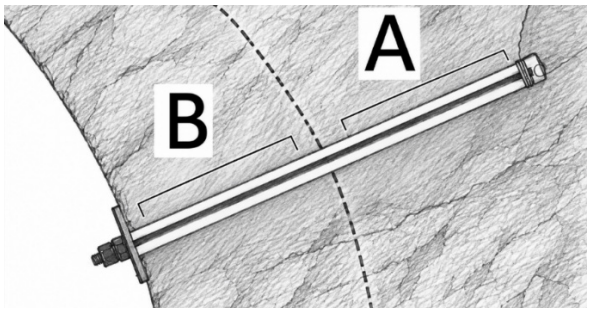


Figure 1 Schematic illustrating rockbolt loading sections during block ejection

In this scenario it is expected that the hybrid bolt will pull free from the rock mass at loads lower than expected, and possibly without the tendon yielding as intended, because insufficient load was transferred via the tendon and was passed along the friction anchor. To the authors knowledge, there is little public data available to support or refute these assumptions.

Dynamic rockbolts are commonly qualified using laboratory impact testing methods intended to simulate in situ seismic loading. The 2 principal approaches are:

- continuous-tube, direct-impact testing, which simulates rock mass strainburst behaviours
- split-tube, indirect impact testing which simulates block ejection scenarios.

This paper presents a series of basic split-tube, indirect impact tests on common mechanical hybrid rockbolt designs from 2 manufacturers to understand if the dynamic capacity published on their technical data sheet (TDS), and derived from continuous-tube tests, can be relied upon as valid for block ejections as well.

2 Mechanical hybrid rockbolt design

Mechanically anchored hybrid rockbolts typically comprise of a full-length friction anchor that encapsulates a yieldable tendon. The tendon material is typically steel with high elongation to failure, ranging 15–27%. For the most common mechanical hybrid bolts, yield loads range 150–180 kN, ultimate tensile loads 210–250 kN, and dynamic capacity for a 2.4 m anchor range 19–60 kJ (Jennmar 2026; Sandvik 2026; Epiroc 2026). A localised mechanical expansion anchor links the tendon to the friction anchor and can be positioned either within the friction anchor, or at its end, see Figure 2.



Figure 2 Examples of common hybrid rockbolt designs (Jennmar 2026; Sandvik 2026; Epiroc 2026)

The mechanically anchored hybrid rockbolts shown in Figure 2 share a common design, installation and application principle. The bolt is installed by mechanised equipment into a pre-drilled support hole ranging 35 to 45 mm in diameter. The compression of the friction anchor causes the bolt to resist insertion into the hole, and therefore percussion is often used to drive the bolt into the hole. Once the faceplate bottoms-out against the rock face, the bolt nut is rotated to activate the mechanical expansion anchor. The expansion anchor typically has a tapered wedge fixed to the bar and one to 2 tapered expansion leaves that are radially fixed within or to the end of the friction anchor. Pulling the tapered wedge into these tapered leaves causes the assembly to radially expand and this pressure against the walls of the borehole creates anchorage.

3 Laboratory impact testing of mechanical hybrid rockbolts

Laboratory-based impact testing is the preferred method to qualify and assess dynamic rockbolt performance, and quantify dynamic capacity specifications to be used on technical documents. Although laboratory testing does not fully represent in situ conditions, it does offer the benefit of test repeatability, safety and reduced cost over in situ testing (Li et al. 2021).

To improve the correlation between laboratory and in situ testing it is common practice to install the rockbolt samples into a host-tube that approximates the boundary conditions of an in situ ground support hole. This is typically achieved through one of 2 methods; the first is to place a cylindrical granite core into 2 half-sections of steel tube, and weld these together to encase and secure the granite core. The second method is to cast cement with aggregate into a steel tube and allow it to cure to full strength (Knox & Hadjigeorgiou 2024). For both methods a support hole is then drilled axially into the assembly and the bolt installed as it would be during normal application. The diameter of the steel tube assembly and the wall thickness, as well as the aggregate–cement mixture strength need to be controlled, such that the radial stiffness of the host-tube approximates what would be common to an in situ support hole drilled into a rock mass.

The 2 most common dynamic impact test machine designs include momentum-transfer and free-falling mass. Both designs impart kinetic energy into an axially aligned rockbolt sample and measure how this energy is absorbed and dissipated by the sample. In a continuous-tube, direct-impact, test configuration the strike surface of the sample is attached to the rockbolt faceplate (Li et al. 2024).

For a split-tube, indirect impact, test configuration the strike surface is fixed to the lower half of the host-tube. The energy is transferred from the sample host-tube into the rockbolt sample in a manner that distributes this energy along the lower encapsulated length of the sample rather than directly onto the faceplate, simulating the loads common to a block ejection event (Knox & Hadjigeorgiou 2024).

The results of these impact tests are typically expressed as force–displacement curves from which an absorbed energy total can be derived. Both test methods are considered to produce comparable results, although each method does provide its own set of benefits and drawbacks (Li et al. 2021). Some typical examples of a dynamic test result graphs are presented in Section 5 of this paper, plotting load versus rockbolt sample deformation against the left axis and absorbed energy versus deformation on the right axis.

4 Test configuration and methodology

4.1 Host-tube preparation

Hybrid bolts rely on frictional anchorage between the bolt and host rock, furthermore the bolt maximises pull-out resistance from the rock by imparting radial pressure along the contact surfaces with the rock. It is therefore critical that laboratory tests simulate the strength, frictional, elastic and stiffness characteristics of a support hole drilled into rock. The typical elastic modulus range for common lithologies found in deep hard rock mines is 50–100 GPa (Gudmundsson 2011). For this investigation a conservative target of 60 GPa is set for the host-tube elastic modulus, and an ultimate compressive strength of 47 MPa representing a fractured, blocky, good quality quartzite rock (Hoek & Corkum 2002).

To simulate the frictional coefficient between the steel bolt and the rock mass, the industry typically relies on casting cement into a steel host-tube (Knox & Hadjigeorgiou 2024). The friction coefficient of clean, smooth steel against a drilled quartzite rock is estimated to average 0.35 (Jonak et al. 2021).

The radial stiffness of a Ø45 mm support hole drilled into 60 GPa rock can be estimated from the classical Lamé/Kirsch circular-opening solution, Equation 1 or by Equation 2 the radial stiffness formula for pressurised cylinders, assuming an infinitely thick wall. Both approaches approximate the radial stiffness of a 45 mm support hole drilled into blocky quartzite to be ~ 2,182 MPa/mm.

$$\boldsymbol{K_r = \frac{E_r}{a(1+\nu)}} \quad (1)$$

$$K_r = \frac{2E}{(1+\nu)}\left\{\frac{d_o^2-d_i^2}{d_i[(1-2\nu)d_i^2+d_o^2]}\right\} \quad (2)$$

where:

K_r = borehole radial stiffness (MPa/mm)

E_r = rock elastic modulus (60 GPa)

d_i = hole diameter (45 mm)

d_o = outer diameter (∞ for in situ holes)

a = hole radius

ν = Poisson's ratio (0.22) (Gerçek 2007).

In summary, the support hole we aim to simulate in this study has an elastic modulus of 60 GPa, a friction coefficient of 0.35, a radial stiffness of 2,182 MPa/mm and a rock medium strength of 47 MPa.

A split-tube style, indirect impact host-tube was designed to match these parameters as closely as possible, see Figure 3. The design comprises of 2 ASTM106 B steel tube sections of 1,240 mm each, and are 139 mm in diameter, with a 5 mm wall thickness. Each steel tube is cast with 40 MPa cement with stone aggregate and allowed to cure 28 days. A diameter 45 mm hole is drilled co-axially into the cured cement using a coring machine and the impact ring is welded to the bottom of the lower host-tube.

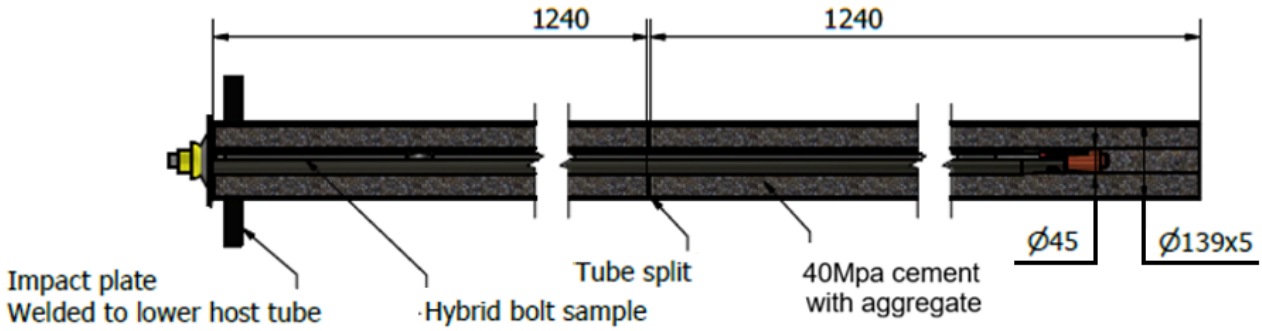


Figure 3 Split type, indirect impact host-tube design

The elastic modulus of the host-tube can be calculated as follows;

Steel tube:

$$A_s = \frac{\pi}{4}\left(139^2 - 129^2\right) = 2105 \text{ mm}^2 \quad (3)$$

Cement annulus:

$$A_c = \frac{\pi}{4}\left(129^2 - 45^2\right) = 11\,480 \text{ mm}^2 \quad (4)$$

Total material area:

$$A_{\text{material}} = 13\,585 \text{ mm}^2 \quad (5)$$

Equivalent axial modulus for bonded materials undergoing equal strain:

$$E_{\text{eq}} = \frac{E_s A_s + E_c A_c}{A_s + A_c}$$

$$E_{\text{eq}} = \frac{(210000)(2105)+(35000)(11480)}{13585}$$

$$E_{\text{eq}} = 62 \text{ GPa} \quad (6)$$

Assuming:

- tube 139 × 129 mm
- central hole diameter = 45 mm
- steel modulus $E_s = 210$ GPa
- concrete modulus $E_c \approx 35$ GPa.

The radial stiffness of the assembly can be estimated from:

$$\boldsymbol{K_r = \frac{2E}{(1+\nu)}\left\{\frac{d_o^2-d_i^2}{d_i\left[(1-2\nu)d_i^2+d_o^2\right]}\right\}}$$

$$\boldsymbol{K_r = \frac{2(210000)}{(1+0.3)}\left\{\frac{139_o^2-129_i^2}{d_i\left[(1-(2*0.3))129_i^2+139_o^2\right]}\right\} + \frac{2(35000)}{(1+0.22)}\left\{\frac{129_o^2-45_i^2}{d_i\left[(1-2(0.22))45_i^2+129_o^2\right]}\right\}}$$

$$\boldsymbol{K_r = 1242\ \mathrm{MPa/mm}} \quad (7)$$

The radial stiffness of the host-tube is 40% below the target of 2,182 MPa/mm, however no practical steel tube combination could be found that would meet these criteria. It was decided to proceed as similar research by Knox & Hadjigeorgiou (2024) was successful with host-tube stiffnesses as low as 705 MPa/mm. The lower than desired stiffness will also impact all tests equally as all samples in this investigation used the same host-tube design.

4.2 Dynamic impact test machine

Normet Asia-Pacific owns and operates a rockbolt test laboratory, which hosts a free-mass style dynamic impact test machine, see Figure 4. The machine is in Perth, Western Australia and has run internal and external testing for the Australian industry for 5-plus years, at a rate of at least one test a month in recent years.

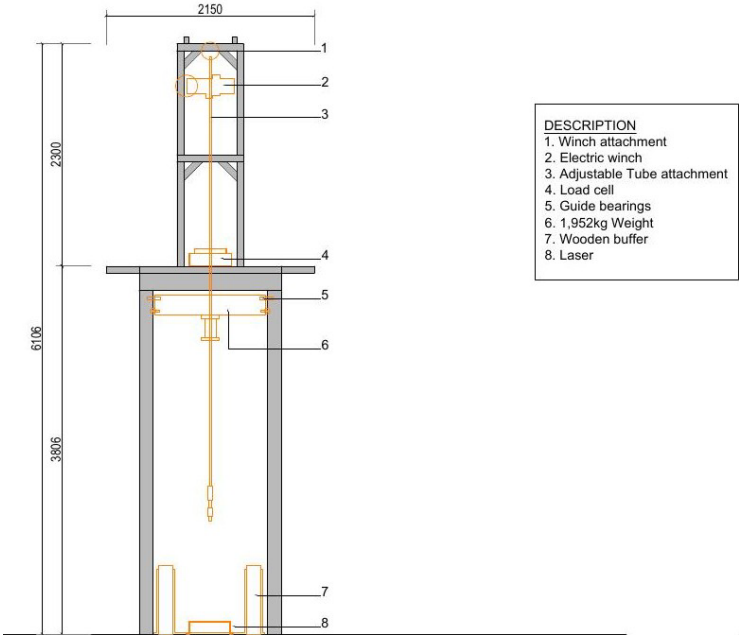


Figure 4 Normet dynamic impact tester – Perth, Western Australia

The machine features a 2,200 kg free-fall mass with a maximum drop height of 2.05 m. The machine is instrumented with a load cell at the top of the test frame from which the host-tube samples are fixed and suspended from. At the base of the machine is a laser displacement sensor that records displacement of the rockbolt sample faceplate. The signals from the 2 data sources are recorded by a 10 kHz data-acquisition system and the data is aggregated and processed by mXrap (Harris et al. 2025). Summarised technical specifications are provided in Table 1.

Table 1 Normet dynamic impact test facility general specifications

Technical specification	
Drop mass range (kg)	1,906–2,262
Drop height (m)	0–2.05 m
Maximum drop velocity (m/s)	~ 6.3
Maximum sample size (mm)	Ø142 × 3,000
Maximum input energy (kJ)	~45

4.3 Sample preparation

A total of 6 sample sets, each comprising 3 sample units, were tested. These sample set are identified as:

- Sample A: split-tube, indirect impact test of sourced Ø46 × 2,400 mm hybrid bolt with internal expansion anchor – 20 mm tendon.
- Sample B: split-tube, indirect impact test of fabricated Ø46 × 2,400 mm hybrid bolt with external expansion anchor – 22 mm tendon.
- Sample C: split-tube, indirect impact test of fabricated Ø46 × 2,400 mm hybrid bolt with external expansion anchor – 28 mm hollow tube tendon.
- Sample D: split-tube, indirect impact test of fabricated Ø46 × 2,400 mm hybrid bolt with external expansion anchor – 28 mm hollow tube tendon and energy release points.
- Sample E: continuous-tube, direct-impact test of sourced Ø46 × 2,400 mm hybrid bolt with internal expansion anchor – 20 mm tendon.
- Sample F: continuous-tube, direct-impact test of fabricated Ø46 × 2,400 mm hybrid bolt with external expansion anchor – 22 mm tendon.

Sample A is sourced from a dominant market supplier of mechanical hybrid bolts. Sample B is a replica of a common, external expansion shell hybrid bolt as no stock of the original equipment manufacturer (OEM) product was available for this study. The sample design features components of similar geometric shape and materials as for the OEM product but features a tendon with a 19% elongation limit rather than the 22% published for the OEM product.

Sample C and D were manufactured by Normet using an R28 SDDB bolt as the tendon, these samples are called HX-Bolt here forth. The R28 SDDB allows the injection of pumpable urea-silicate resin into the installed assembly. The R28 SDDB is a hollow dynamic bolt designed to accommodate resin or grout injection through the bolt. It has an outer diameter of 28 mm, inner diameter of 17 mm, a yield limit of 180 kN, ultimate tensile strength of 250 kN and an elongation limit of 19%. A 2.4 m length sample has the capacity to absorb 60 kJ. Samples C and D feature an external expansion shell design like the design of sample B but adapted to accommodate the R28 tendon.

Sample D is shown in Figure 5, and is similar to sample C but features slots cut into the friction anchor at intermittent spacing with the intension to limit the tensile capacity of the friction anchor without compromising radial stiffness, or the compressive push-out resistance the friction anchor uses to resist unwanted movement of the expansion end-anchor mechanism within the bore.

Sample E is a continuous-tube, direct-impact test of sample A. The test acts as confirmation the OEM bolts perform to the specifications published by the OEM for continuous-tube, direct-impact dynamic tests, when tested in the method published by this study.

Sample F is a continuous-tube, direct-impact test of sample B. The test acts both as confirmation the replica bolt performs like the OEM model it is based on, and as a control sample to confirm the design of the host-tube can replicate performance results published for the external expansion anchor style hybrid bolts.

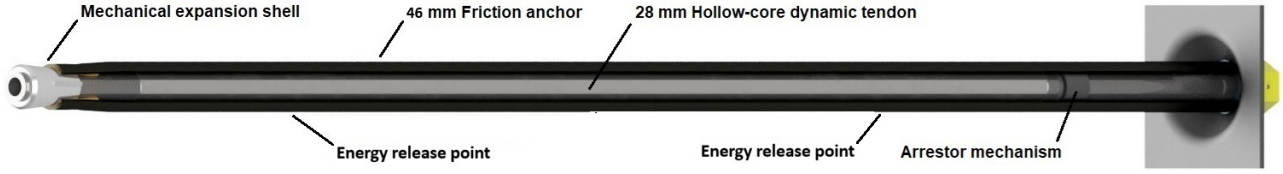


Figure 5 Normet HX-Bolt (45 × 2,400 × 28 mm Groutable Hybrid Bolt)

The samples were installed into host-tubes using a percussive feed bench installed in the Normet rockbolt testing facility, simulating installation by a mechanised bolting machine. Nuts were pre-tensioned to 350 Nm using a manual torque-wrench.

Samples C and D were then injected with standard Portland cement and allowed to cure for 7 days before testing. The grout was injected through the hollow core of the tendon until resin became visible at the bolt faceplate, ensuring full encapsulation was achieved.

5 Results

All samples were dynamically testing using the same input energy of 38 kJ achieved by a drop weight of 2,228 kg released from 1.75 m above the impact plate.

5.1 Sample set A

Testing of the samples with the internal expansion mechanism resulted in the units pulling free from the upper host-tube. Referring to the results in Figure 6, the initial load uptake is progressive and peaks at an average of 180 kN and ~40 mm faceplate displacement before the anchor fails. Only one sample generated data before failure and no controlled yield of the tendon is observed, although the peak load recorded is equivalent to the typical yield load of the tendon.

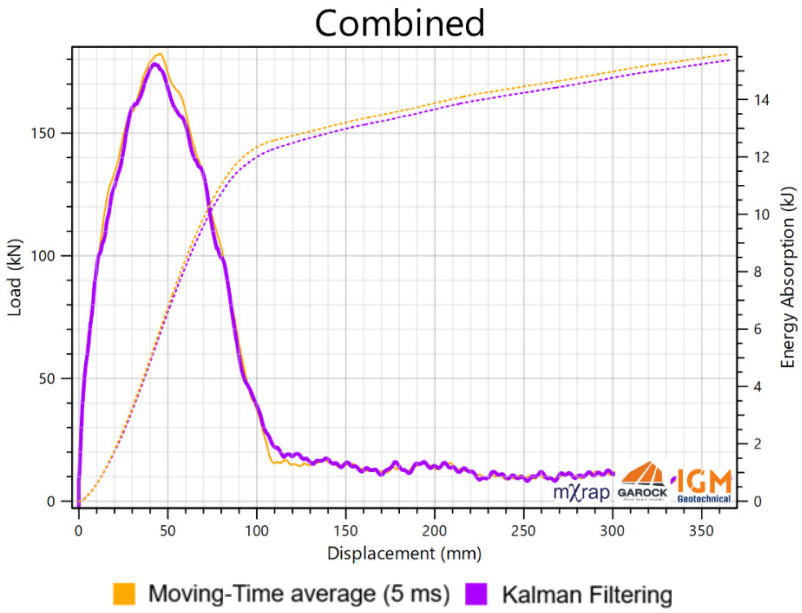


Figure 6 Sample set A: Test one – load versus displacement versus energy curve

5.2 Sample set B

Testing of the samples with the external expansion mechanism resulted in 2 samples failing due to the units pulling free from the upper host-tube. The results of one such test are presented in Figure 7 and show the initial load uptake is progressive and peaks at an average of 130 kN and ~50 mm faceplate displacement before the anchor fails. Again, the peak load is approaching the typical yield limit published in the supplier's TDS. Test sample 3 was able to maintain anchorage into the upper host-tube, and the results are shown in Figure 8. A total energy of 39.44 kJ was successfully arrested over a displacement of 184 mm. The system appears to yield after 60 mm of displacement was recorded, after which a load of ~250 kN was maintained over the remaining 124 mm of displacement.

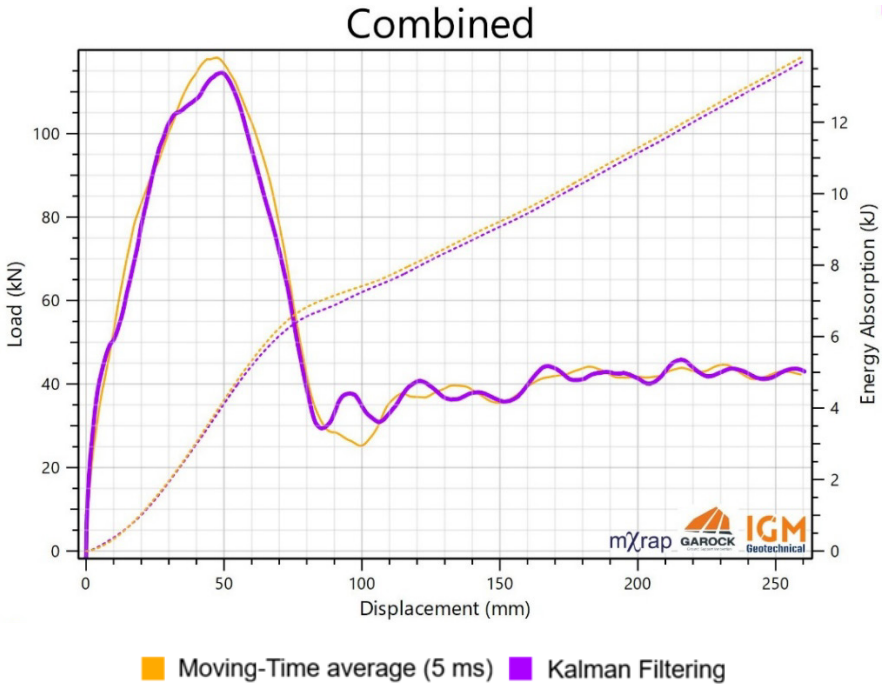


Figure 7 Sample set B: Test 2 – load versus displacement versus energy curve

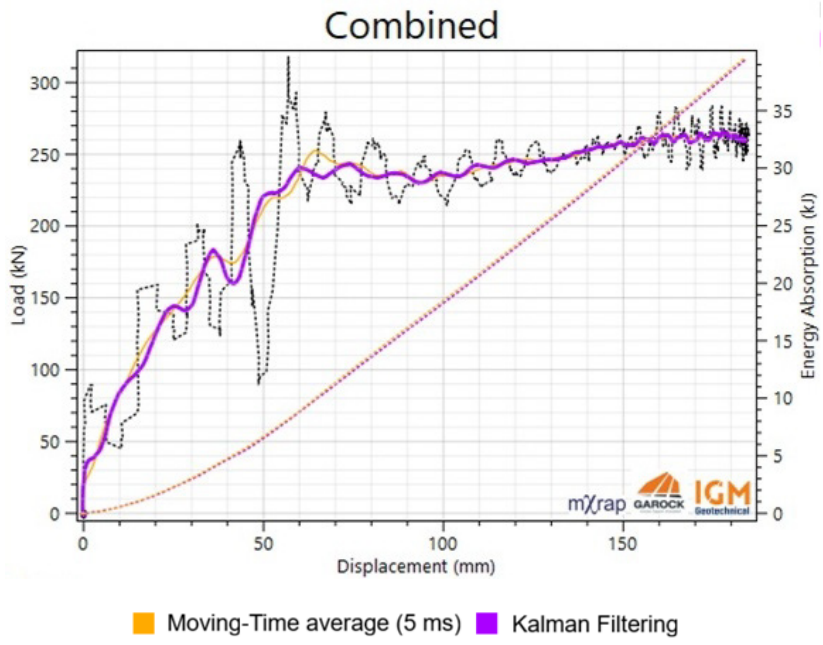


Figure 8 Sample set B: Test three 3 – load versus displacement versus energy curve

5.3 Sample set C

The HX-Bolt samples without the energy release points consistently absorbed the energy impulse without failure of the anchor and were able to support the drop mass after release. Referring to Figure 9, Peak loads observed during this test were 345 kN, where the tendon ultimate tensile strength (UTS) were 250 kN suggesting the friction anchor is contributing the tensile capacity of the anchor. Total elongation averaged slightly over 100 mm. The initial load uptake is somewhat erratic with good initial stiffness observed up to 180 kN, followed by a sudden drop in load, which is then recovered as loads build to the peak of 335 kN. The stiffness of the system appears reduced after the load dips at 180 kN with greater displacement recorded per unit increase in load, than prior to the dip 35 kN/mm versus 6.7 kN/m. Total supported load reduces gradually as displacement increases from 40 mm onwards.

Inspection of the tested samples showed that the 150 × 150 × 6 mm faceplate had collapsed during testing, indicating forces greater than 150 kN were transferred onto the faceplate during testing. The friction anchor is intact in spite of the 108 mm displacement of the bolt. It was not possible to measure the end position of the bolt before and after testing, so it is not possible to quantify how much of the displacement is anchor slippage versus controlled tendon yield.

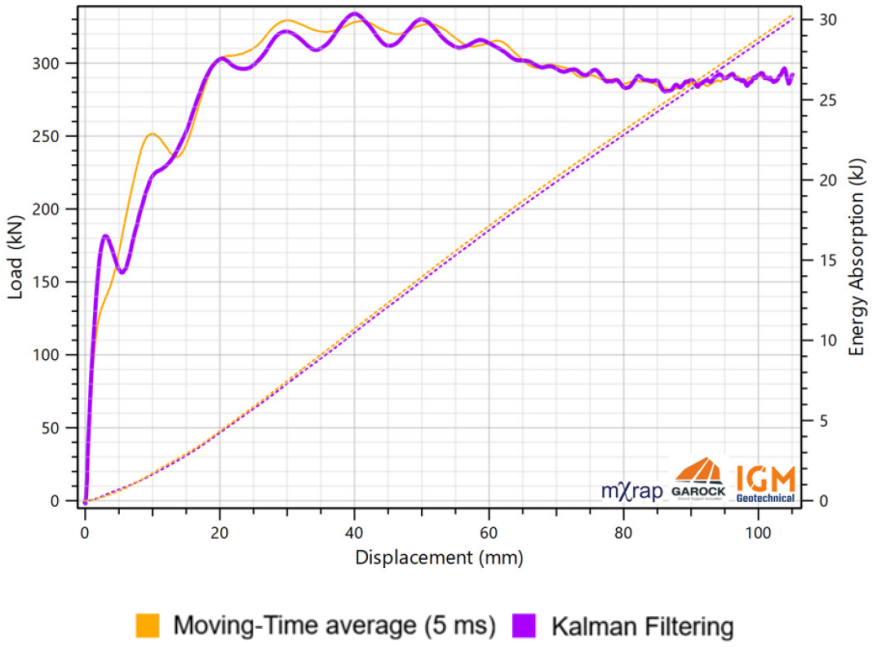


Figure 9 Sample set C: Test one – load versus displacement versus energy curve

5.4 Sample set D

The HX-Bolt samples with the energy release points consistently absorbed the energy impulse without failure of the anchor and were able to support the drop mass after release. Referring to Figure 10, peak loads observed during this test were 260 kN, slightly higher than the tendon UTS of 250 kN. Total elongation averaged 130 mm. The initial load uptake is progressive and stiff, 44 kN/mm. At 220 kN, there is a dip in the bolt's resistance and a displacement of 10 mm before the load is recovered and builds to its peak of 260 kN with a stiffness of 4 kN/mm. This peak load is then maintained evenly throughout the remaining 100 mm of bolt displacement before bringing the drop mass to rest. Inspection of the samples showed the friction anchor failed around the separation point between the 2 host-tubes, exposing the elongated bolt tendon, see Figure 11. The faceplates were observed to still be in their original form, with no signs of collapse suggesting faceplate loads were below 170 kN during testing.

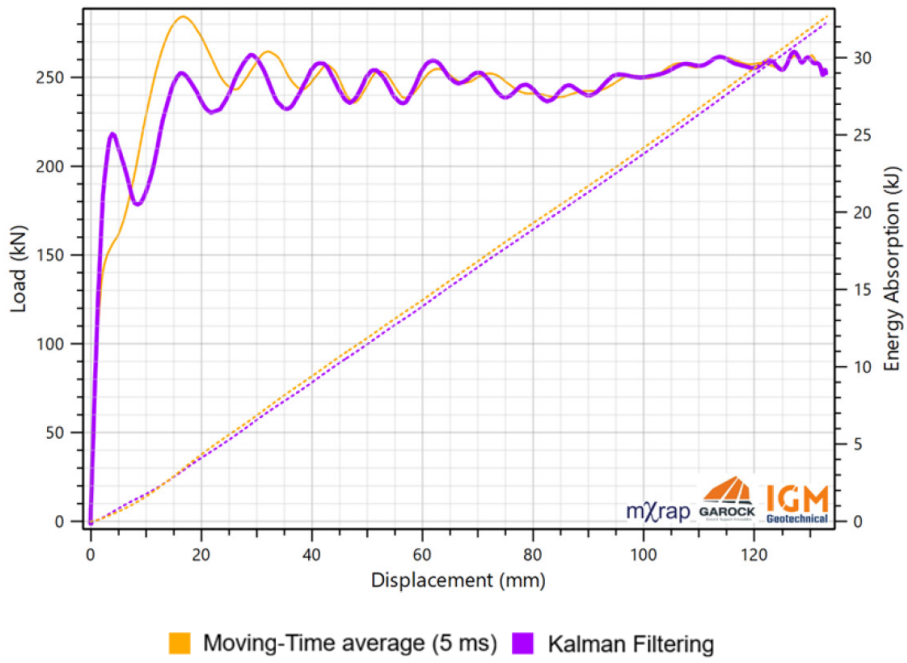


Figure 10 Sample set D: split-tube separation



Figure 11 Sample set D: Test one – split-tube separation

5.5 Sample set E

All 3 samples failed to arrest the 38 kJ impulse. Inspection of the samples indicated failure of the expansion anchor mechanism occurred on all 3 samples, with no samples arresting more than 9 kJ of energy before this failure.

5.6 Sample set F

All 3 samples tested in sample set E successfully arrested the dynamic impact impulse. Inspection of the friction anchor position at the collar of the borehole confirmed that no friction anchor slippage had occurred and that all displacement achieve by the bolt can be attributed to the plastic elongation of the tendon. The test also confirms that the design of the host-tube, in terms of cement strength and assembly stiffness, is compatible with the design of the anchor and the bolt can perform to OEM specification in such a host-tube. The test results published in Table 2 are compared with the results published by Knox & Hadjigeorgiou (2024)

for a similar style hybrid bolt. In their study, the test samples elongated ~142 mm after a dynamic impulse of 32 kJ. The initial load development rate in their study range 9–13 kN/mm of displacement until the yield limit is achieved.

Figure 15 shows a slack initial load development rate of approximately 4.2 kN/mm where the testing by Knox & Hadjigeorgiou (2024) achieved 9–13 kN/mm. Referring to Table 2, the fabricated samples elongated ~164 mm when subjected to similar input energy. Given the tendon material used for sample set B has an elongation slightly less than published for the OEM model, yet 13% more displacement occurred and a slack initial load development is seen, it suggests there was anchor slippage in these tests that may not have been present in the tests by Knox & Hadjigeorgiou (2024). It is noted that in those tests 90 MPa cement was cast into the host-tubes, where for these tests 40 MPa with aggregate was used.

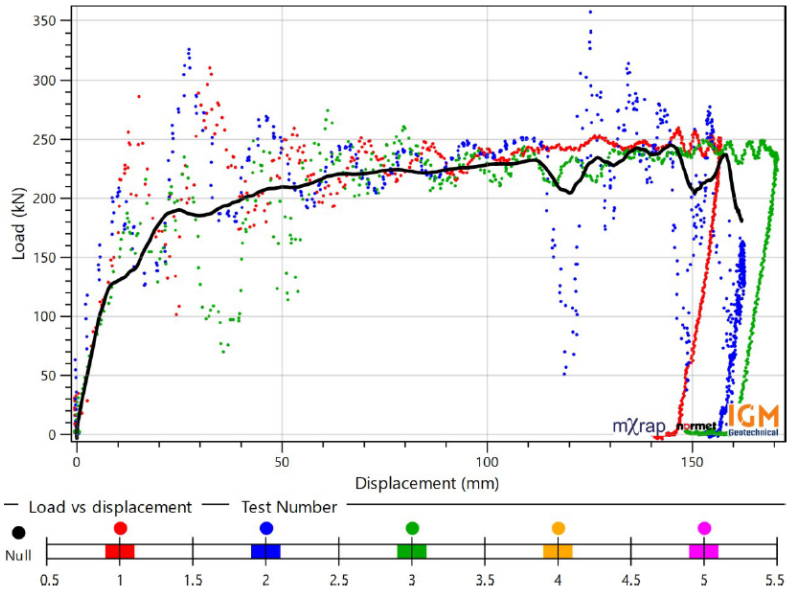


Figure 15 Test results table for sample set E: continuous-tube, direct-impact test of sample B style bolt

Table 2 Test results table for sample set E: continuous-tube, direct-impact test of sample B style bolt

Parameter	Sample 1	Sample 2	Sample 3	Combined
Drop height (m)	1.45	1.45	1.45	1.45
Mass (kg)	2,262	2,262	2,262	2,262
Theoretical impact velocity (m/s)	5.33	5.33	5.33	5.33
Energy absorption (kJ) Moving-time window	33.7	33.4	33.7	33.6 ± 0.2
Energy absorption (kJ) Kalman filter	33.4	33.1	33.4	33.3 ± 0.2
Maximum displacement (m)	157	163	171	164 ± 7
Total fall height (m)	1.61	1.61	1.62	1.61 ± 0.01
Potential energy (kJ)	35.7	35.8	36.0	35.8 ± 0.2

Given the investigation is not comparing elongation properties across the sample set, the fabricated samples used in test set B will be used to represent the industry standard hybrid bolt with an external expansion mechanism, but it is noted the host-tubes used may cause less stiff load development and could be causing anchor slippage due to a softer cement being cast.

6 Discussion

6.1 Anchorage and load transfer mechanics

The pull-out resistance of common 47 mm split-set bolts can be assumed to average 40kN/m length in common hard rock (Villaescusa & Wright 1997; Tomory & Grabinsky 1998). The bolt samples presented in this study were installed with approximately symmetric embedment lengths into the upper and lower host-tube. We can therefore assume the friction anchor component offers about 48 kN anchorage into each half of the host-tube. The expansion element anchored into the upper host-tube ensures the distal end of the bolt has greater anchorage than the proximal side anchored into the lower host-tube.

The anchorage of the friction anchor into the lower tube section is overcome at ~48 kN, whereafter the lower host-tube will slip over the bolt and transfer impact load onto the faceplate. This localised slippage and load transfer onto the faceplate should increase tension onto the expansion mechanism, increasing its traction into the upper host-tube. We expect the only difference in performance between continuous-tube and split-tube dynamic test result to be an offset in the yield load equivalent to the force required to overcome the frictional bond of the lower host-tube, ~48 kN. Beyond this the general mechanism suggests that mechanically anchored hybrid rockbolts should perform well in split-tube indirect impact tests.

6.2 Observed failure mechanisms

The results achieved in sample set A show that the initial load development rate is about 4.5 kN/mm of displacement up to a peak load of 180 kN, after which the units pull free of the upper host-tube. Continuous-tube, direct-impact testing of a similar bolt by Darlington et al. (2023) shows dynamic curves where initial load development rates are 13–18 kN/mm of displacement. Similar initial load development rates are achieved for the control sample test E of this bolt continuous, direct-impact testing. The slower load development rate of sample set A and inspection of the samples confirm the anchor is slipping within the upper host-tube. However, anchorage capacity is increasing over time, in spite of the reducing embedment length into the upper host-tube, suggesting load is being transferred to the faceplate by the lower host-tube, and the expansion anchor is progressively developing anchorage.

In sample set B, 2 units failed in a similar manner as for sample set A. Load builds progressively until ~50 mm of displacement is achieved, after which the confinement load is spontaneously lost. The peak load achieved is 130 kN, lower than sample set A, but both samples A and B failed at approximately the same faceplate displacement of 50 mm. Initial load development is significantly less than achieved in the testing of samples A and E, with 2.7 kN/mm of displacement. The final sample from set B was able to arrest 39.44 kJ of energy without failure. The initial resistance to load development appears similar as for the continuous-tube test of this bolt design, sample set F, but is still considered slack, averaging 4.36 kN/mm displacement. This is similar to the initial load development rate achieved for sample set A.

Samples A, B, F and E form the control baseline for the study. It is noted that the test design appears to be causing slacker initial load development than is published by the OEM suppliers. However, sample set F confirms the bolts from sample set B can consistently perform to specification when tested in this method; in a continuous-tube, direct-impact test method. Regarding the testing of hybrid bolts with an internal expansion mechanism, the OEM performance could not be replicated in continuous-tube test format, nor was a successful test achieved in split-tube format. Although useful insight is gathered from test A and E regarding peak loads and initial load development rates, the remainer of the study will focus on hybrid bolt designs with an external expansion mechanism.

6.3 Factors influencing favourable energy absorption

Comparing the testing from samples B and F, load development rates differ significantly yet the design of the bolt is identical. In continuous-tube format initial load develops at 4.36 kN/mm but in split-tube testing only at 2.7 kN/mm. In the continuous-tube test of sample F the anchorage contribution of the friction anchor is

~96kN (40 × 2.4 m) as the full length of the friction anchor is embedded into competent ground. In the split-tube test sample B only ~48 kN (40 × 1.2) is anchored into competent ground and needs to resist the pull-out force being generated by the equal length anchored into the displacing lower host-tube. Given the host-tubes of this test are symmetric, the friction anchorage into the upper and lower host-tubes are equal and cancel each other out to provide no net contribution to anchoring the bolt assembly into the competent rock. The expansion mechanism is therefore required to support the system capacity alone, whereas in a continuous-tube test it would be aided by ~96 kN of anchorage capacity provided by the full length of the friction anchor.

The success of one unit in sample set B confirms the expansion anchor can achieve sufficient anchorage to support the system in a split-tube test if load transfer onto the faceplate develops favourably during testing. This requires the slip of the anchor within the host-tubes to be biased towards the lower host-tube. Adequate pre-tensioning of the bolt to fully activate the expansion mechanism may be the deciding factor in directing this bias, but also in situ bulking may reduce the effective anchorage of the lower portion of the bolt to achieve this balance.

Results are expected to improve significantly if the position of the host-tube split is moved lower down toward the faceplate to favour anchorage length into the competent rock, highlighting depth of block ejection is highly relevant to the performance of a mechanically anchored rockbolt. It is clear that a critical bond length does exist for mechanically anchored hybrid rockbolts and it is likely greater than half the embedded length of the bolt.

6.4 Evaluation of alternative hybrid bolt designs

In an effort to improve the critical bond length required by mechanically anchored hybrid bolts, Normet has designed the HX-Bolt to offer the same functions and attributes of a typical dynamic mechanical hybrid bolt, but with the additional feature of accommodating the injection of grout or resin into the bolt to further enhance anchorage capacity.

The results presented for sample set C show the increase in anchorage is greatly enhanced with the inclusion of a grout, allowing all 3 samples to pass the split-tube test. However, the conflicting load path along the friction anchor remains undesirable because the loads required to yield the bolt are excessive, ~300 kN , and the yield profile is not well controlled. There may be benefit in avoiding the friction anchor slippage mechanism to transfer load to the faceplate for the grouted configuration of such a hybrid bolt.

Sample set D avoids the friction anchor slippage mechanism by including a series of precision slots (energy release points) punched into the friction anchor at intermittent spacing along its length. The sizing of these slots is such that they limit the tensile capacity of the friction element to a controlled threshold, without reducing the resistive push-out force of the component from the hole. That is, the end-anchor expansion mechanism benefits from the same push-out resistance from the friction anchor as is available in sample set C, despite the tensile capacity of the friction anchor being limited.

An example of the test results for this system is shown in Figure 13. Initial load development is comparatively stiff at 44 kN/mm of displacement. Release of the friction anchor energy release points occurs at 220 kN, within 5 mm of bolt displacement. Once the anchor transitions all load to the internal tendon, the yield load is well controlled and stable, holding at approximately 250 kN until the mass is arrested at 130 mm of displacement.

7 Future work

This study has focused on results from laboratory testing only and does not fully consider the influence that in situ loading may have on the performance of the tested samples. Future work should include a more thorough understanding of how pre-tension of the expansion shell influences the bolt's critical bond length for both split-tube testing and general block ejection scenarios. Similarly, the influence of rock mass bulking needs to be better understood in the context of how much tensile load is ultimately applied to the bottom length of the bolt friction anchor during a seismic block ejection event. Bulking may reduce the tensile force

applied to the friction anchor, thereby reducing the magnitude of the conflicting load path along the friction anchor into the competent rock.

This study has also not presented a continuous-tube test of HX-Bolt once grouted. Once encapsulated with grout, the threads along the proximal length of the bolt are bonded to the grout, isolating the loads from the smooth yielding section of the tendon. The bolt can therefore only plastically yield once this bond has been overcome and broken, placing unwanted stress on the system components. This has been considered in the design by limiting the length of thread on the proximal side of the bolt and placing an energy release point into the friction anchor close to the proximal end of the bolt. However, confirmation testing will follow to confirm the solution performs.

It will be beneficial to quantify the short-encapsulated quasi-static pull-out resistance of the bolts presented in this paper to understand if the concerns around block-ejection capacity is limited to dynamic or also quasi-static load scenarios.

8 Conclusion

For common mechanically anchored hybrid bolts, the friction anchor component is highly beneficial to enhance anchorage into the host rock without the use of resins or grouts. It offers a rapid installation cycle, can be installed with a variety of equipment and is suitable to varied ground conditions. However, this investigation suggests a 2.4 m long bolt requires anchorage into competent rock well exceeding 1,200 mm depth before it can provide reliable dynamic support for block ejections or similar scenarios. This critical bond length may be variable and driven by the specific bolt length, as the system requires the correct balance in anchorage along the friction anchor to work. The quantification of this is necessary future work. To the authors knowledge, this nuance of the product is not communicated on any supplier TDS or well understood by end-users of these products. The study does suggest that the dynamic performance specifications of these bolts is only applicable if the critical bond length conditions are met and that these critical bond lengths are not clearly defined.

The HX-Bolt provides a potential solution by including post-encapsulation and a novel feature to limit conflicting load paths along the friction anchor. The solution allows operations to rapidly install a full capacity mechanical anchor, as they would with any other hybrid bolt, but can then return later to encapsulate with grout or resin, if desired, to improve safety and longevity of the support. This work can be done safely and without time sensitivity as the mechanical system provides full capacity.

References

Cai, M & Kaiser, PK 2022, 'Selecting the "right" rockbolts for burst-prone drifts', in M Diederichs & J Tshisens (eds), *RaSiM10: Proceedings of the 10th International Symposium on Rockbursts and Seismicity in Mines*, Society for Mining, Metallurgy & Exploration, Englewood, pp. 1–13, https://www.geo-kaiser.ca/www.geo-kaiser.ca/wp-content/uploads/Publications/RASIM22%20Cai%20and%20Kaiser%20the%20right%20bolt%20-0213.pdf

Darlington, B, Vallati, O & Young, P 2023, 'A comparison between laboratory and in situ dynamic testing on the MDX bolt', in J Wesseloo (ed.), *Ground Support 2023: Proceedings of the 10th International Conference on Ground Support in Mining*, Australian Centre for Geomechanics, Perth, pp. 361–370, https://doi.org/10.36487/ACG_repo/2325_24

Epiroc n.d., *Vulcan Bolt*, viewed 23 June 2026, https://www.epiroc.com/en-au/products/rock-drilling-tools/ground-support/energy-absorbing-rockbolts/vulcan-bolt

Gerçek, H 2007, 'Poisson's ratio values for rocks', *International Journal of Rock Mechanics and Mining Sciences*, vol. 44, no. 1, pp. 1–13, https://doi.org/10.1016/j.ijrmms.2006.04.011

Gudmundsson, A 2011, *Rock Fractures in Geological Processes*, Cambridge University Press, Cambridge, https://doi.org/10.1017/CBO9780511975684

Hadjigeorgiou, J & Potvin, Y 2011, 'A critical assessment of dynamic rock reinforcement and support testing facilities', *Rock Mechanics and Rock Engineering*, vol. 44, no. 5, pp. 565–578, https://doi.org/10.1007/s00603-011-0155-4

Harris, PC & Wesseloo, J 2015, *mXrap*, version 5, computer software, Australian Centre for Geomechanics, The University of Western Australia, Perth, https://mxrap.com

Hoek, E, Carranza-Torres, C & Corkum, B 2002, 'Hoek–Brown failure criterion – 2002 edition', in R Hammah, W Bawden, J Curran & M Telesnicki (eds), *NARMS-TAC 2002: Mining and Tunnelling Innovation and Opportunity: Proceedings of the 5th North American Rock Mechanics Symposium and the 17th Tunnelling Association of Canada Conference*, vol. 1, University of Toronto

Press, Toronto, pp. 267–273, https://www.rocscience.com/assets/resources/learning/hoek/2002-Hoek-Brown-Failure-Criterion.pdf

Jennmar n.d., *Mech-Lok Bolt*, viewed 3 July 2026, https://www.jennmar.com/products/mech-lok-bolt

Jonak, J, Karpiński, R, Wójcik, A & Siegmund, M 2021, 'The influence of the physical-mechanical parameters of rock on the extent of the initial failure zone under the action of an undercut anchor', *Materials*, vol. 14, no. 8, article 1841, https://doi.org/10.3390/ma14081841

Knox, G & Hadjigeorgiou, J 2024, 'Direct impact load tests on mechanical hybrid rockbolts', in P Andrieux & D Cumming-Potvin (eds), *Deep Mining 2024: Proceedings of the 10th International Conference on Deep and High Stress Mining*, Australian Centre for Geomechanics, Perth, pp. 467–478, https://doi.org/10.36487/ACG_repo/2465_26

Knox, G & Hadjigeorgiou, J 2025, 'Rockbolts in shear', *Journal of the Southern African Institute of Mining and Metallurgy*, vol. 125, no. 11, pp. 621–628, https://doi.org/10.17159/2411-9717/822/2025

Li, CC 2010, 'A new energy-absorbing bolt for rock support in high stress rock masses', *International Journal of Rock Mechanics and Mining Sciences*, vol. 47, no. 3, pp. 396–404, https://doi.org/10.1016/j.ijrmms.2010.01.005

Li, CC, Hadjigeorgiou, J, Mikula, P, Knox, G, Darlington, B, Royer, R, … Hosp, M 2021, 'Performance of identical rockbolts tested on four dynamic testing rigs employing the direct impact method', *Journal of Rock Mechanics and Geotechnical Engineering*, vol. 13, no. 4, pp. 745–754, https://doi.org/10.1016/j.jrmge.2021.01.003

Li, CC, Mikula, P, Hadjigeorgiou, J, Simser, B, He, M, Canbulat, I & Joughin, W 2024, 'ISRM suggested method for determining the properties of rock bolt assemblies by mass freefall impact testing in the laboratory', *Rock Mechanics and Rock Engineering*, vol. 58, no. 1, pp. 165–179, https://doi.org/10.1007/s00603-024-04159-z

Morissette, P & Hadjigeorgiou, J 2017, 'The development of a ground support design strategy for deep mines subjected to dynamic-loading conditions', in J Wesseloo (ed.), *Deep Mining 2017: Proceedings of the Eighth International Conference on Deep and High Stress Mining*, Australian Centre for Geomechanics, Perth, pp. 651–665, https://doi.org/10.36487/ACG_rep/1704_44_Morissette

Sandvik n.d., *MD/MDX Bolt*, viewed 3 July 2026, https://www.mining.sandvik/en/products/ground-support/bolts-and-cables/friction-bolts/md--mdx-bolt/

Shakeri, J, Ghorbani, E & Taheri, A 2026, 'A review of deep mining challenges, hazard mitigation, design approaches, and support methods', *Underground Space*, vol. 28, no. 3, pp. 86–136, https://doi.org/10.1016/j.undsp.2025.10.011

Tomory, PB, Grabinsky, MW, Curran, JH & Carvalho, J 1998, 'Factors influencing the effectiveness of Split Set friction stabilizer bolts', *CIM Bulletin*, vol. 91, pp. 205–214, https://www.onemine.org/documents/factors-influencing-the-effectiveness-of-split-set-friction-stabilizer-bolts

Villaescusa, E & Wright, J 1997, 'Permanent excavation support using cement grouted split set bolts', *The AusIMM Proceedings*, vol. 302, no. 1, pp. 65–69, https://www.ausimm.com/publications/conference-proceedings/the-ausimm-proceedings-volume-302-no-1/permanent-excavation-support-using-cement-grouted-split-set-bolts/